Airplane Ground Vibration Testing – Nominal Modal Model Correlation

Charles R. Pickrel, Boeing Commercial Airplane Group, Seattle, Washington

A brief overview is given of transport airplane ground vibration testing (GVT) at Boeing Commercial Airplane Group. A GVT is a modal test conducted for the purpose of validating and improving a structural dynamic model of the airplane. A "small signal" model is quickly and conveniently identified from multi-input burst random excitation. Sine excitation is used selectively to adjust the model to account for moderate departure of the airplane from linearity.

Linear structural dynamic models of transport airplanes are used to represent and predict vibrating behavior. When coupled with aerodynamic models, they are used to predict flutter and dynamic loads. The structural dynamic model is validated by comparing its predicted modes with the experimental modes identified from a GVT (see Figure 1).

The airplane structure is modeled in the tested configuration, including support system, fuel and payload mass properties, and with landing gear down. This validated model is then modified to represent various in-flight configurations and a variety of failure conditions. The structure of transport airplanes is found to depart weakly to moderately from linear behavior, so one issue is to identify a 'nominal' linear model (or models) which are representative (and predictive) of the operating structure. We consciously impose the assumption of linearity upon the test structure.

Test Strategy

The approach described here has evolved only moderately from previous testing,[1,2] with the notable addition of multiple inputs,[3,4] and the adjustment for departures from linearity described below. With improvements in pre-test design, instrumentation and especially computing hardware and software, high quality results are obtained quickly.

Our strategy is to identify a linear "small signal" model (borrowing terminology from electrical engineering), and adjust it according to amplitude dependencies that are identified from selective sine testing. An important issue is whether the small signal model is representative of the structure in operation. If a structure is not linear and random excitation does not excite relevant mechanisms in the structure, then some form of either sine or operating excitation must be employed.[5-9] In the case of transport airplanes, the small signal modal model is appropriate for our purposes and has been reported by other authors.[10-12]

Testing time on a new model airplane is very expensive. Our approach to the GVT aims to shorten the test time consistent with quality results, and with uncertainty and accuracy that are consistent with the needs of our modeling predictions.[13] A summary of our strategy:

- Pretest design and preparation.
- Soft support boundary conditions.
- Linearize test structure.
- Small signal model from multiple-input-multiple-output (MIMO) burst random FRFs.
- Amplitude dependencies from selective sine tests.
- Validation of experimental model, including redundant data set.

Design for Success

Pre-test planning and design play an important role in facilitating the efficient conduct of a GVT. This process was previously described in detail[14] and is only briefly summarized here. The test analysis model is used to assure that sensors and exciters are well located. FRFs are synthesized and parameter estimation is performed in a simulation of the test. Excitation hardware is checked for possible dynamic interaction with the structure. The support system is designed and modeled to assure its performance. Drawings and workbooks are prepared to facilitate sensor installation.

A set of 250 to 320 sensors is located to provide mode shape visualization and expansion, and to include the set (one per mode) indicated by effective independence of the mode shapes from the pre-test model.[15,16] Shown in Figure 2 on the left are 50 sensors (shown displaced) located by effective independence from a generous (but reduced) set of model locations. On the right, additional sensors have been added for a total of 256 locations.

One approach to selecting input locations is to take the product of all modal coefficients,[14,17] the result of which is shown

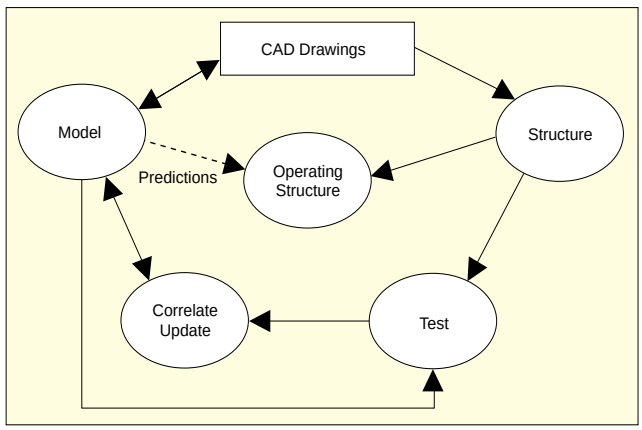

Figure 1. Validation map for structural dynamic model.

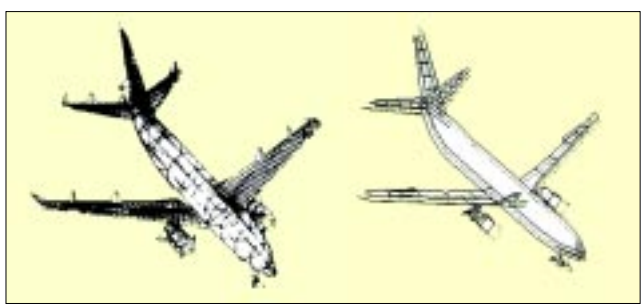

Figure 2. (left) Location of 50 sensors (shown displaced) from 50 modes, using effective independence. (right) Full set of 256 sensors provides mode visualization.

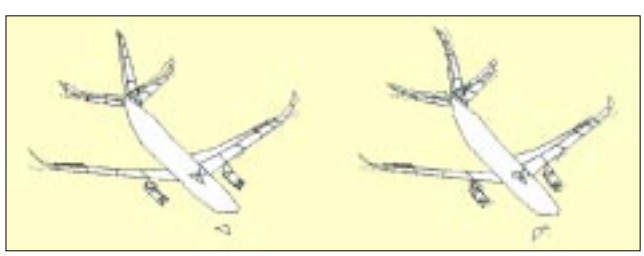

Figure 3. (left) Product of modal coefficients shows where all modes may be excited. (right) Average of driving point residues.

Based on a paper presented at IMAC-XX the 20th International Modal Analysis Conference, Los Angeles, CA, February 2002.

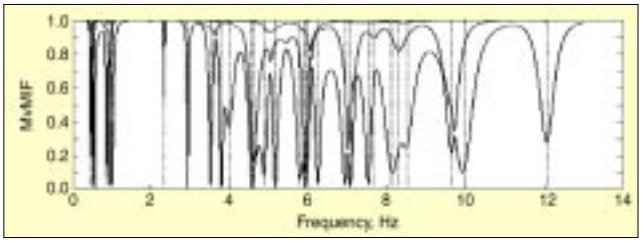

Figure 4. MvMIF of synthesized FRFs shows how easily modes will be identified from candidate input locations.

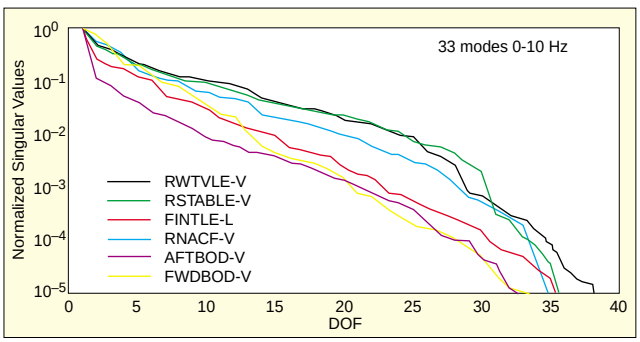

Figure 5. Modal energy distribution from individual candidate input locations.

on the left in Figure 3. This product goes to zero at node lines for any mode. Not surprisingly, this favors locations near the "free ends" of the airplane lifting surfaces. Additional candidate locations may be selected from the average driving point residues,[18] shown on the right in Figure 3.

FRFs are synthesized from the pre-test model (using assumed damping) for a number of candidate input locations for shakers. Mode indicator functions are computed and locations are selected that will identify modes based on the value of the indicator function[19] as shown in Figure 4. This process, which amounts to a simulation of the modal test, helps the test engineer become familiar with the model and facilitates the correlation effort. The distribution of energy across the modes is shown in Figure 5 for individual candidate locations.

Additional considerations for selecting input locations (not discussed here) include the spatial independence of multiple input locations, shaker attachment hardware and impedance issues, and the decay times for burst random signals. In practice, we try to minimize the number of locations in the interest of saving test setup time. A typical test will use two configurations of four inputs each. The second set is considered redundant insurance for validation purposes. If modes are missed in the parameter estimation, we are prepared to add additional inputs.

Boundary Conditions

It is desired to provide "free-free" boundary conditions to the airplane to the greatest practical extent. To this end, the system in Figure 6 was designed and built to lift the airplane inches above the floor on a soft cushion of air (see front cover). The effectiveness of this system in separating the rigid modes from flexible modes is shown in Figure 7 which contrasts the FRFs of the airplane sitting on tires vs. softly supported by this system. On the tires the rigid and flexible modes are coupled, while the soft support effectively separates them.

The support system is not perfect, however, as it has moving mass and modes of its own. By design, the dynamics of the support system do not couple with the important flexible modes of the airplane. This is illustrated in Figure 8, which shows the cross MAC comparing the soft-supported modes vs. the free-free modes of the flexible modes of the airplane (from the pre-test analysis).[20]

Linearize the Structure

We consciously impose our assumption of linearity upon the

Figure 6. Soft support (shown under right main landing gear), floats airplane inches from floor.

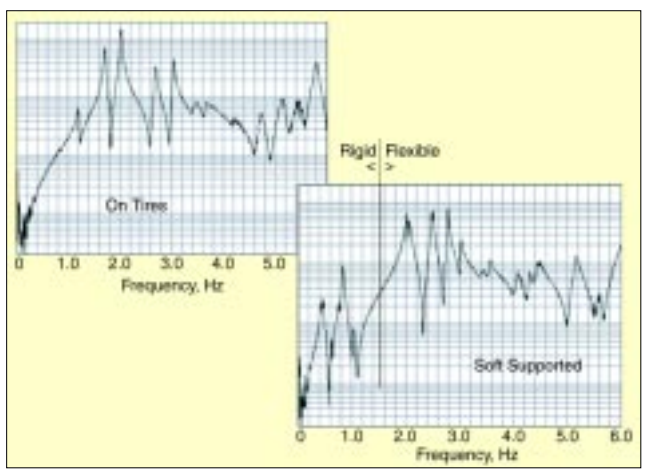

Figure 7. Soft support effectively separates rigid modes from flexible modes.

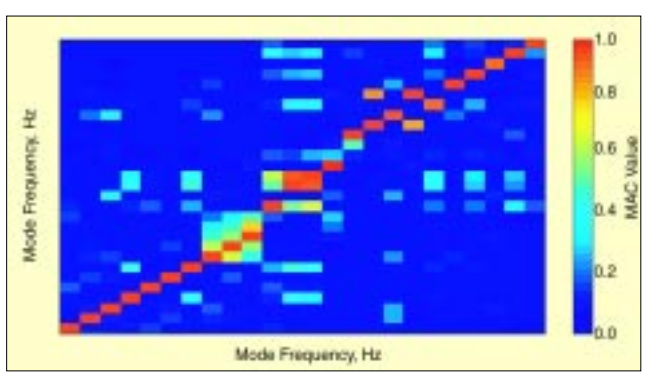

Figure 8. MAC compares analysis mode shapes for soft-supported (y) vs. free-free (x). New modes are added, but important structural modes are unaffected.

structure in an attempt to produce the 'cleanest' possible linear FRFs. This will allow the estimation of a modal model to proceed quickly and without ambiguity. Where appropriate, soft pre-load is applied through a bungee support system simulating normal operation. Most significantly, multiple input, low level, burst random excitation is used with ensemble averaging. All data are acquired simultaneously. Low noise transducers and instrumentation are used.[21]

Sample Test Results

Examples of FRF magnitude are shown in Figure 9 from a four shaker MIMO burst random data set in the frequency range of 1 to 25 Hz. The data shown are from a wing tip vertical input. The responses are at wing tip vertical (driving point) and body nose fore-aft, which represent the highest and lowest response locations. The vertical axis spans 5 decades starting at 10^{-6} g/lb. This frequency band encompasses about 65 flexible

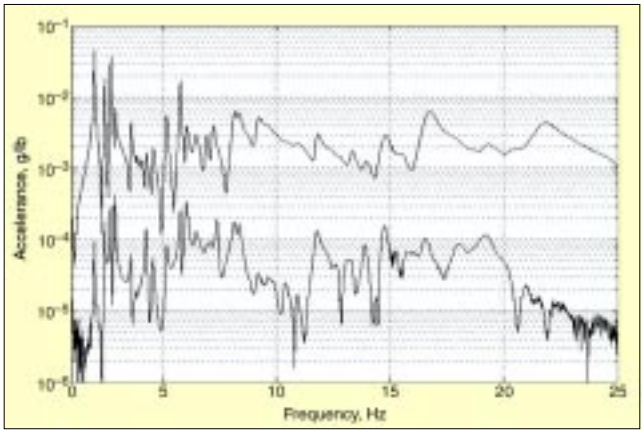

Figure 9. Typical FRFs of a transport airplane, showing highest (wing tip Z) and lowest (body nose X) response locations. MIMO burst random excitation.

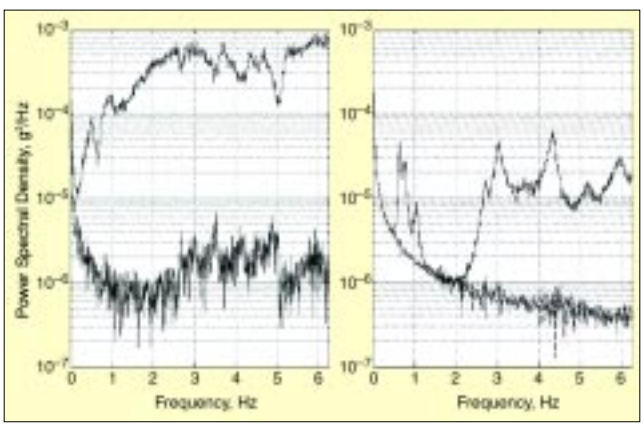

Figure 10. Response spectrum and noise floor : (left) wing tip Z; (right): body nose X.

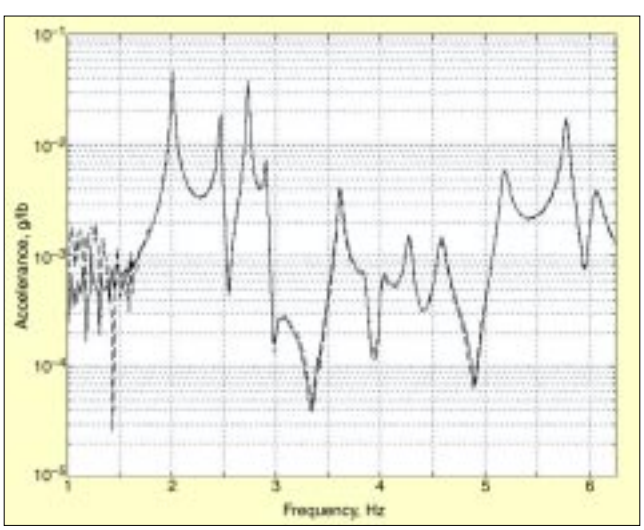

Figure 11. Reciprocal FRFs from wing tip to wing tip are nearly identical from the burst random excitation.

airplane modes.

The graphs in Figure 10 compare the response spectra of the same two sensors with their noise floor, in the frequency range of 0 to 6.25 Hz. The response is an averaged power spectrum measured during a four-input MIMO test with burst random excitation. The noise floor is a single (no average) power spectrum measured with the shakers turned off.

The wing tip sensor shows some response to environmental excitation. Note that the bottom of these graphs represents 1/10 micro-g. Excellent reciprocity is demonstrated by comparing the wing tip to wing tip measurements, which are almost indistinguishable in Figure 11. The frequency range shown is

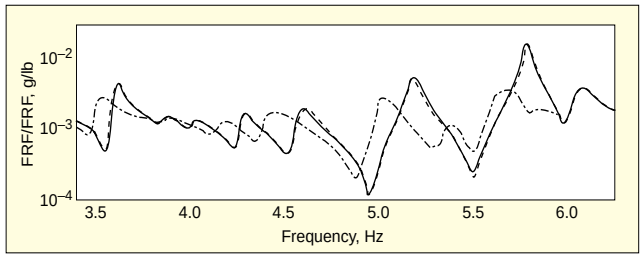

Figure 12. Wing tip driving point FRFs: (solid) random; (dashed) low-level sine; (dot-dash) high-level sine.

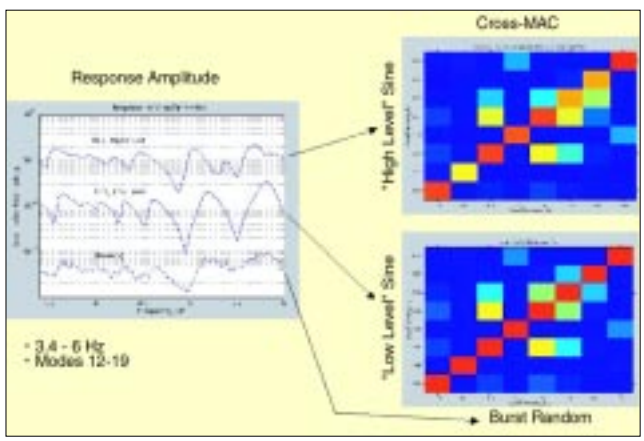

Figure 13. Comparison of mode shapes derived from measurements at different force and response amplitudes. Mode shapes vary little or none with amplitude.

1-6.25 Hz. Efforts to linearize the airplane structure and produce high quality FRFs were successful. This greatly facilitates the identification of a modal model. There are 13 flexible modes shown from 2 to 6.25 Hz.

Departures from Linearity

At this stage, a general treatment of modal testing should assess the linearity of the test structure in the context of the application. From experience we know that our small-signal model, obtained from the MIMO burst random test, will not be fully representative of our in-flight airplane. We investigate modes involving flexibility of the engine nacelle struts, some of which are important to our prediction of flutter. This is a built up structure, which contains pinned joints and typically exhibits stiction effects.

Two approaches of single input sine testing are applied to identify the amplitude-dependence of the structure:

1. Stepped sine 'sweeps' define FRFs at many frequencies, and a few different amplitudes.
2. "Mini sweeps" define FRFs at a few frequencies in vicinity of a single mode, repeated at many steps in decreasing amplitude.

In each case, a (linear) modal model is fit to the FRF data to identify adjustments which may be needed to the small signal model to represent behavior of the airplane at higher amplitudes.

Stepped Sine. FRFs were measured using single input sine excitation, with steady state measurements performed at each discrete frequency. In this example, two force levels were used in the 3.4 to 6 Hz range. The overall (time domain) response level was approximately the same during the low-level sine excitation as it was during the 4 input random excitation. The response to the high-level sine excitation would have been sufficient to spill drinks in the cabin. Wing tip driving point FRFs are compared in Figure 12 for three different excitation cases. The burst random (solid line) and low-level sine (dashed line) are nearly identical. The high-level sine shows significant changes in mode frequency and damping. There are 8 modes in the 3.4 to 6.0 Hz band. A ninth mode is found at 6.07 Hz in

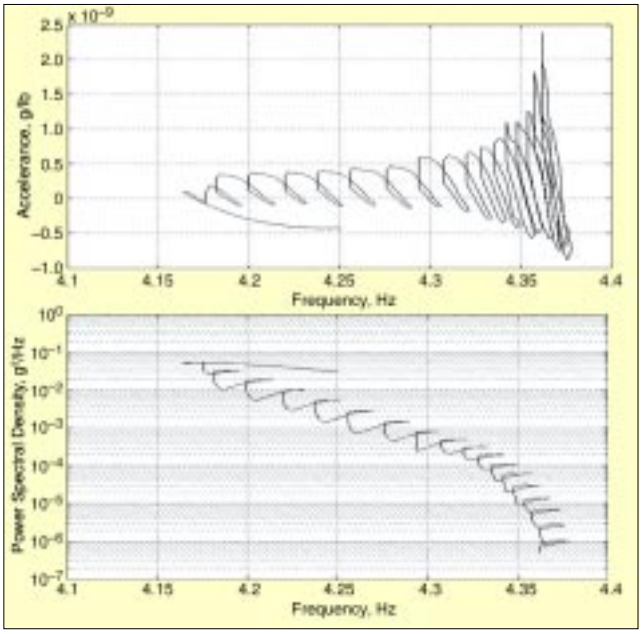

Figure 14. A single mode is tracked with "mini-sweeps"as amplitude is varied. (top) Real part of FRF, (bottom) response amplitude.

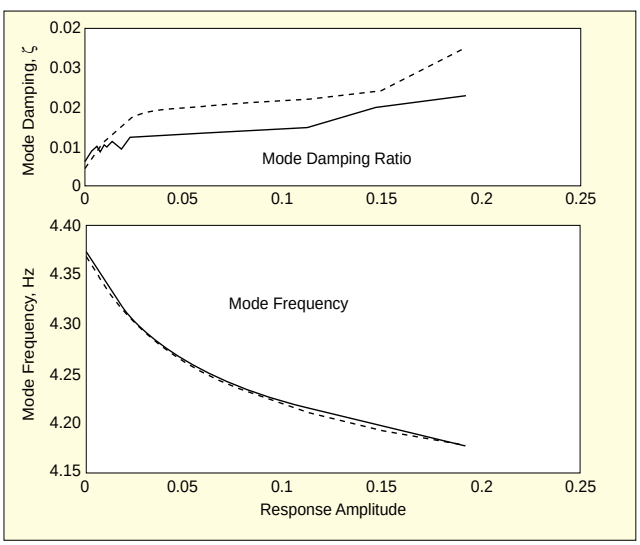

Figure 15. Variations of mode frequency and damping with response amplitude. Both "sweep up" and "sweep down" results are shown.

the random data, and falls below 6 Hz in the high-level sine measurement.

A modal model was estimated from each set of sine FRFs and compared with the small signal (MIMO random) model. The resulting shapes for the 8 modes from 3.4 to 6 Hz are compared in Figure 13. Also shown are the corresponding response power spectrum magnitudes. Note that the response amplitude was allowed to vary; no control loop was applied. The mode shapes are mostly unaffected by response amplitude. Some change is found in the nacelle lateral bending mode (second from left). Virtually no change is seen in the important wing + nacelle vertical mode (fourth from left).

Mini-Sweeps. Another approach is to perform the discrete sine measurements in such a way as to measure only a few frequencies at each of many amplitudes. Special software called 'SMART' (Sinusoidal Modal Analysis and Resonance Tuning) is used to control acquisition. A stepped measurement performs both a "sweep up" and "sweep down" in the vicinity of a desired mode at a high amplitude. The amplitude is successively reduced and the 'sweep' process is repeated at each amplitude, defining the FRF at a minimum of 5 frequencies in the vicinity of the mode frequency. A least squares single degree of freedom (SDOF) approach[22] is used to identify the mode

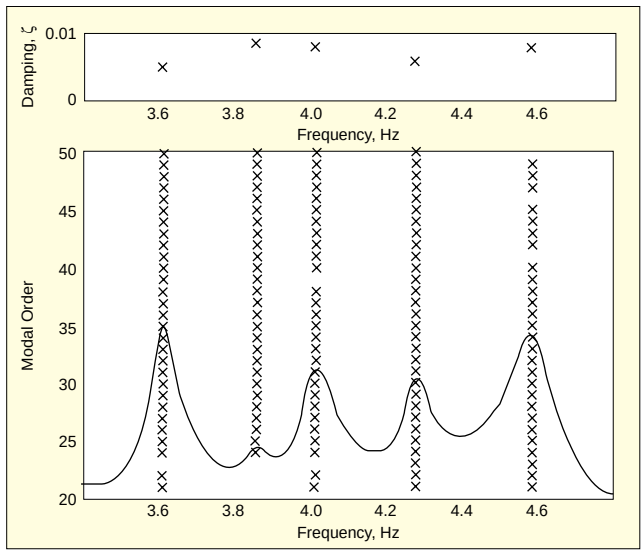

Figure 16. Pole surface and consistency diagram for data from MIMO burst random excitation indicate ease of model identification.

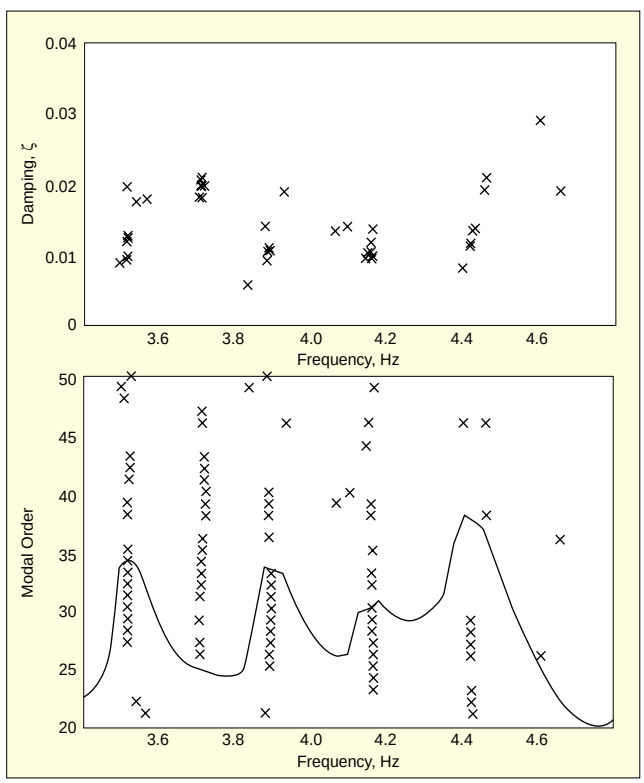

Figure 17. Pole surface and consistency diagram for data from high-level sine excitation suggest ambiguity in model identification.

at each amplitude.

An example is shown in Figure 14, which shows the real part of the FRF vs. frequency (top), and the logarithmic response amplitude vs. frequency (bottom). The mode frequency and damping are shown as a function of response amplitude in Figure 15. While the mode shape does not change (MAC greater than 0.99) the frequency drops about 3% and the damping increases dramatically, when comparing the small signal model to high amplitude sine measurements.

The mini-sweep process in this example was used to define the amplitude dependence of four important modes of interest: modes number 7, 10, 13 and 15, at frequencies from 2 to 4.2 Hz. Each mode required 60 to 100 measurement points. The stepped sine FRF (at one amplitude from 3.4 to 6 Hz) required 105 points. The single input approach has worked surprisingly well for this purpose when both input and response locations are well chosen. It could be applied to multiple shakers in

symmetric pairs to isolate individual modes, but this has not been necessary on our airplanes.

Advantage of Linearization. In a previous section, we compared the FRF data from the MIMO burst random excitation with that obtained by single input stepped sine. If we require a modal model that is relevant to operating response amplitude, why are we measuring a small signal model in the first place? Why not perform modal analysis using excitation to high response levels? In this example, using modern time and frequency domain parameter estimation algorithms,[23] we find it is a great deal easier to estimate a (linear) modal model using FRFs from the MIMO burst random excitation. We illustrate by 'fitting' the 5 modes between 3.4 and 4.7 Hz from the above example. Figure 16 shows the pole surface and consistency diagram plots[24,25] generated from the MIMO burst random FRFs. Identifying a modal model is very straight forward using this data and can be done quickly. Furthermore, the acquisition time for the sine data can be far greater than the time required for a burst random data set.

Similar plots are shown in Figure 17 using the FRFs from the high-level stepped sine excitation. These data appear very 'noisy' due to the fact that the airplane structure is no longer linear at these amplitudes and the FRFs contain non-linear distortion.

Limits to Correlation

In Figure 18 the shapes of 33 modes up to 10 Hz are compared using the MAC between the predictions of the analysis model (x axis) and the test-derived mode shapes (y axis). The important flexible modes agree quite well and for the purpose of predicting flutter, this correlation is excellent. The correlation of shapes in this example goes "out of focus" at higher frequencies after 20 or so modes.

At even higher frequencies, we find the non-linearity of the structure renders linear modal analysis impractical. We compare modal models from two different levels of excitation in the mid frequency range in Figure 19. (Note: This example is taken from a different airplane test than the previous examples.) The FRFs and mode shapes from a small-signal random test are compared with those derived from a higher level sine sweep test. Note the shapes compared are for mode numbers 34 to 47. Only a few of these modes have similar shapes. For the most part one would say there is no unique modal model (derived by linear modal analysis) to describe this structure at these frequencies. Similar differences in mode shape occurred when comparing data from sine sweeps at two different levels of excitation. Note that the FRFs remain substantially similar.

Test Model Validation

We wish to validate our identified modal model. One approach is to synthesize FRFs and compare them to measurements as shown in Figure 20. The shapes of 54 test modes are compared using the MAC in Figure 21. Three mode pairs appear similar and deserve closer scrutiny, but is this a good modal model? We re-computed these same 54 mode shapes using the same poles but different frequency bands of the FRF data. Two of the example sets of shapes are compared in Figure 22. We find there are a number of mode shapes that we cannot estimate consistently and a number of the highest frequency modes were wishful thinking. Fortunately, the modes of greatest interest were quite consistent.

We also find that many of the modes whose shapes were not consistent were local modes of the soft support system. This reveals the compromises that were made in the test design. For economic reasons, the input locations on the soft support system structure were not used and these local modes received little energy from the input locations that were used.

Another consideration for our test modes is mode shape complexity. Polar plots are shown for 54 test modes in Figure 23. An ideal normal mode should appear as a single vertical line. The important flexible modes are actually quite good. The

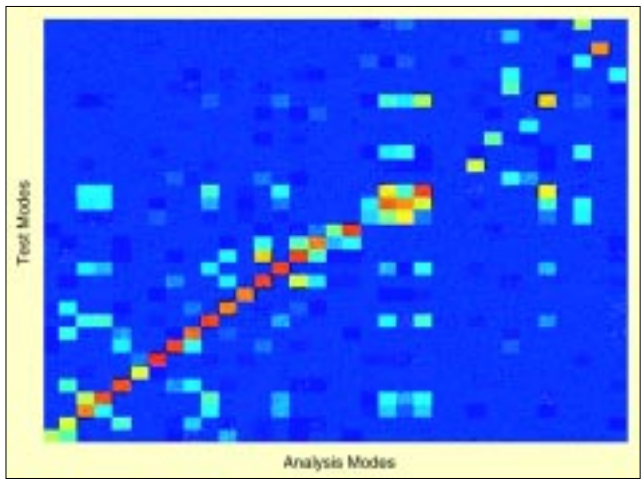

Figure 18. MAC compares mode shapes of analysis model vs. test. About 20 modes correlate, departing at higher frequencies.

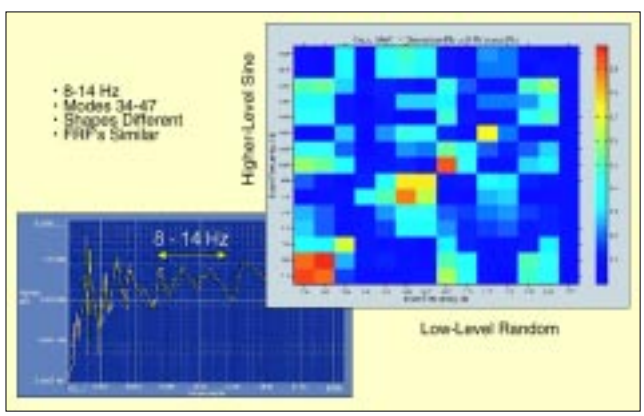

Figure 19. Modal models derived from high-level and low-level excitation at mid frequencies. Most shapes are different, while FRFs are similar (these data are taken from a different, larger airplane).

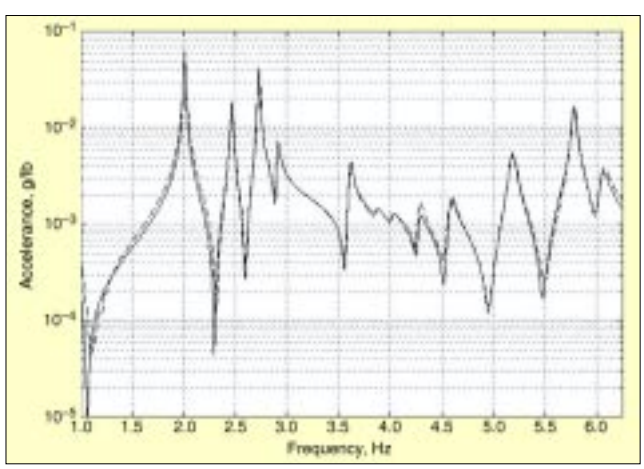

Figure 20. Sample comparison of: (dashed) measured FRF, with (solid) function synthesized from test modal model.

first 6 modes are rigid body modes occurring from 0.4 to 1.03 Hz and reveal phase shifts due to transducer and instrumentation time constant mismatch. The local support system modes (which were not consistent in the shape comparison of Figure 22) display a high degree of complexity. These local modes were not well excited and are "under represented" in the sensor set.

Conclusion

We have shown and discussed the GVT of a transport airplane. As part of test preparation and design, the GVT was simulated using the pre-test analysis model. The airplane departs moderately from linearity which is a predominant source

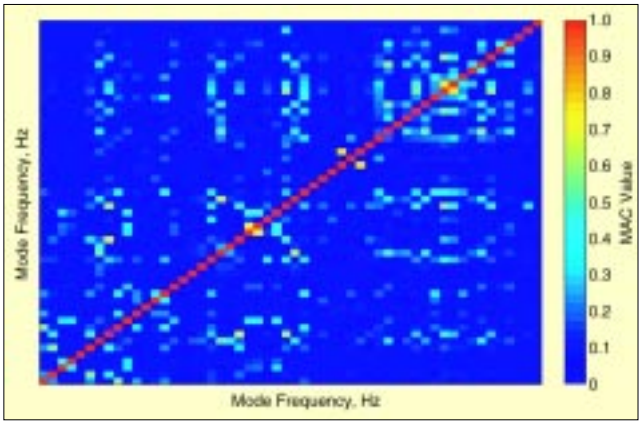

Figure 21. Auto MAC of 54 mode test model.

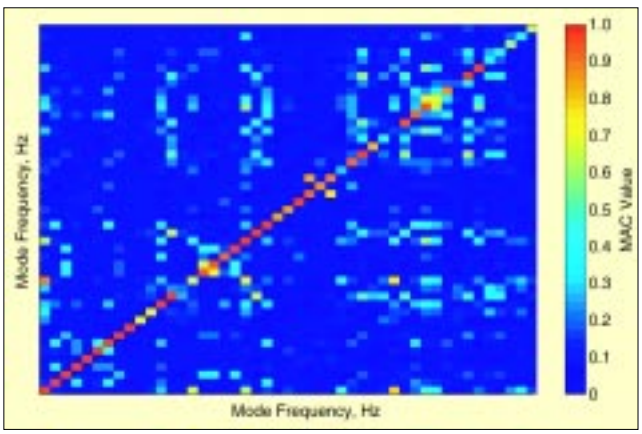

Figure 22. MAC compares shapes estimated from same poles using different FRF frequency subsets. Some modes could not be estimated

Figure 23. Polar plots of test modes reveal complexity and 'noise' on some modes.

of uncertainty in our use of a linear model for structural dynamic prediction. We made every reasonable attempt to make the structure linear for testing, including a soft support system for boundary conditions. A small-signal model was identified from FRFs measured using MIMO burst random excitation.

Adjustments to the small signal model were identified by selective single input sine testing. FRFs were measured using discrete stepped 'swept' sine at a few amplitudes and a modal model was fit to these data. The backbones of individual modes were identified by fitting a linear SDOF model, piece-wise to mini-sweeps of a few frequencies (near the mode frequency) at each of many amplitudes. With increasing response amplitude, some mode frequencies dropped, mode damping increased and most mode shapes were unaffected. An important decision of the analyst is to select a nominal linear model (or models) to support necessary prediction in the operating environment.

The test model was evaluated for self consistency and at least 20 of the analysis modes correlated well. At higher frequencies, above 30 or 40 modes, the structure defies linear modal analysis.

References

1. Dotson, B. F., Brown, D. L., Michalak, R. F., Allemang, R. J., and Gimmestad D., "Optimum Ground Vibration Test Method," AFWAL contract F33615-77-C-3059, 1979.
2. Olsen, N. and Walters, M., "747 Space Shuttle Carrier Aircraft/Space Shuttle Orbiter Mated Ground Vibration Test: Data via Transient Excitation and Fast Fourier Transform Analysis," SAE Paper No. 770970, Nov 14-17, 1977.
3. Allemang, R. J., "Investigation of Some Multiple Input/Output Frequency Response Function Experimental Modal Analysis Techniques," Ph. D. thesis, Dept. of Mech. & Indust. Eng., University of Cincinnati, 1980.
4. Carbon, G., Brown, D. L., and Allemang, R. J., "Application of Dual Input Excitation Techniques to the Modal Testing of Commercial Aircraft," Proceedings of the 1st International Modal Analysis Conference, 1982.
5. Olsen, N. "Excitation Functions for Structural Frequency Response Measurements," Proceedings of the 2nd International Modal Analysis Conference, 1984, pp. 894-902.
6. Lewis, R., and Wrisley, D., "A System for the Excitation of Pure Natural Modes of Complex Structures," *J. Aeronautical Sci.*, Vol. 17, No. 11, 1950, pp. 705-722.
7. Dieckelman, R. J., "Modern Sine Excitation GVT Techniques," Proceedings of the 20th International Modal Analysis Conference, Los Angeles, 2002.
8. Ewins, D. J., *Modal Testing: Theory and Practice*, Research Studies Press, 1991.
9. Allemang, R. J., Brown, D. L., and Rost, R. W., "Experimental Modal Analysis and Dynamic Component Synthesis," Wright Aeronautical Laboratories Report AFWAL-87-3069, 1987.
10. Leppert, E., Lee, S., Day, F., Chapman, B., and Wada, B., "Comparison of Modal Test Results: Multipoint Sine Vs. Single Point Random," SAE paper 831435, 1976.
11. Gimmestad, D., "Your Next Ground Vibration Test Doesn't Have to Cost a Million Dollars," AIAA paper 810528, 1981.
12. Hunt, D., "A Comparison of Methods for Aircraft Ground Vibration Testing," Proceedings of the 3rd International Modal Analysis Conference, Orlando, 1985, pp. 131-137.
13. Pickrel, C., "Testing for Model Validation in Structural Dynamics - Where Idealization Meets Reality," Proceedings of the Seventh International Conference on Recent Advances in Structural Dynamics, Southampton, July 2000, pp. 21-38.
14. Pickrel, C. R., "A Practical Approach to Modal Pretest Design," Mechanical Systems and Signal Processing, V. 13, No. 2, 1999, pp. 271-295.
15. Kammer, D. C., "Sensor Placement for On-Orbit Modal Identification and Correlation of Large Space Structures," *AIAA Journ. of Guidance, Control and Dynamics*, Vol. 14, No. 2, pp. 251-259, 1991.
16. Schedlinski, C., and Link, M., "An Approach to Optimal Pick-up and Exciter Placement," Proceedings of the 14th International Modal Analysis Conference, Dearborn, 1996.
17. De Clerck, J. P. and Avitable, P., "Development of Several New Tools for Modal Pre-Test Evaluation," Proceedings of the 14th International Modal Analysis Conference, Dearborn, MI, pp. 1272-1277, 1996.
18. Jarvis, B., "Enhancements to Modal Testing Using Finite Elements," *Sound and Vibration*, pp. 28-30, Aug., 1991.
19. Carne, T. G., and Dohrmann, C. R., "A Modal Test Design Strategy for Model Correlation," Proc. 13th Intl. Modal Analysis Conf., Nashville, 1995, pp. 927-933.
20. Allemang, R. J., and Brown, D. L., "A Correlation Coefficient for Modal Vector Analysis," Proc. 1st Intl. Modal Analysis Conf, Orlando, Florida., pp. 110-116, 1982.
21. Foss, G., "Measurement System Noise," Proceedings of the 20th International Modal Analysis Conference, Los Angeles, 2002.
22. Phillips, A., and Allemang, R. J., "Single Degree of Freedom Modal Parameter Estimation Methods," Proc. of the 14th Intl. Modal Analysis Conf., 1996.
23. Allemang, R. J., Brown, D. L., and Fladung, W., "Modal Parameter Estimation: A Unified Matrix Polynomial Approach," Proc. of the 12th Intl. Modal Analysis Conf., Honolulu, pp. 501-514, 1994.
24. Phillips, A., and Pickrel, C., "Philosophy, Design, Implementation and Application of Modal Analysis Software System," Proc. of the 12th Intl. Modal Analysis Conf., Honolulu, 1994.
25. Phillips, A., Allemang, R. J., and Pickrel, C., "Clustering of Modal Frequency Estimates from Different Solution Sets," Proc. of the 16th Intl. Modal Analysis Conf., 1997.

SV

The author can be contacted at: charlie.pickrel@boeing.com.